Published in final edited form as:
Ophthalmic Surg Lasers Imaging Retina. 2014 ; 45(5): 382–389. doi:10.3928/23258160-20140909-08.

Swept-source OCT Angiography of the Retinal Vasculature using Intensity Differentiation Based OMAG Algorithms

Yanping Huang, PhD[*,1], **Qinqin Zhang, PhD**[*,1], **Mariana Rossi Thorell, MD**[2], **Lin An, PhD**[3], **Mary Durbin, PhD**[3], **Michal Laron, PhD**[4], **Utkarsh Sharma, PhD**[3], **Giovanni Gregori, PhD**[2], **Philip J. Rosenfeld, MD, PhD**[2], and **Ruikang K Wang, PhD**[§,1,5]

[1]Department of Bioengineering, University of Washington, Seattle 98195, WA

[2]Department of Ophthalmology, Bascom Palmer Eye Institute, University of Miami Miller School of Medicine, Miami, 33136, FL

[3] Advanced Development Group, Carl Zeiss Meditec, Inc., Dublin, 94568, CA

[4]Clinical Affairs Group, Carl Zeiss Meditec, Inc., Dublin, 94568, CA

[5]Department of Ophthalmology, University of Washington, Seattle, 98104, WA

Abstract

Background and Objective—To demonstrate the feasibility of using a 1050 nm swept-source OCT (SS-OCT) system to achieve noninvasive retinal vasculature imaging in human eyes.

Materials and Methods—Volumetric datasets were acquired using a ZEISS 1 μm SS-OCT prototype that operated at an A-line rate of 100 kHz. A scanning protocol designed to allow for motion contrast processing, referred to as OCT angiography or optical microangiography (OMAG), was used to scan ~3 mm × 3 mm area in the central macular region of the retina within ~4.5 seconds. Intensity differentiation based OMAG algorithm was used to extract 3-D retinal functional microvasculature information.

Results—Intensity signal differentiation generated capillary-level resolution *en face* OMAG images of the retina. The parafoveal capillaries were clearly visible, thereby allowing visualization of the foveal avascular zone (FAZ) in normal subjects.

Conclusion—The capability of OMAG to produce retinal vascular images was demonstrated using the ZEISS 1 μm SS-OCT prototype. This technique can potentially have clinical value for studying retinal vasculature abnormalities.

INTRODUCTION

Healthy microcirculation in the retina and choroid is of critical importance for normal vision. Vision threatening retinal diseases such as diabetic retinopathy (DR), age-related macular degeneration (AMD), retinal vein occlusion, and macular telangiectasia often

[§]Corresponding author: Ruikang K Wang, PhD, 3720 15th Ave NE, Box 355061, Seattle, 98195, WA, wangrk@uw.edu.
[*]Equal contributing authors.

involve the retinal microvasculature. Therefore, there is a need to develop noninvasive clinical imaging tools that can assess the health of the microcirculation in the retina.

Currently, there are a number of imaging technologies available in the ophthalmic clinics that are frequently used to examine the posterior pole such as color fundus photography (FP), fluorescence angiography (FA), indocyanine green angiography (ICGA) and optical coherence tomography (OCT).[1, 2] FP is widely used clinically as a screening tool to identify and stage a disease and monitor its progression. However, the limited resolution of FP, its inability to monitor blood flow and the need for stereoscopic viewing to obtain depth-resolved information render it inadequate for providing routine assessment of the retinal microvasculature. FA is widely available and historically considered to be the gold standard for diagnosing vascular diseases of the retina. Furthermore, it has the added value of being able to show leakage from the abnormal retinal microvasculature and from neovascularization. However, FA is not ideal for observing the choroidal vasculature because of the absorption of the excitation/emission light by the retinal pigment epithelium (RPE). Consequently, ICGA was developed to better visualize the choroidal vasculature using an infrared light that allows for deeper penetration into the choroid. However, in spite of the proven clinical utility of FA and ICGA for the diagnosis of retinal vascular diseases, there are some critical factors that make their use less desirable on a regular basis in clinics. The difficult workflow of the dye-based injection approach used in FA and ICGA, the time, the cost, and the potential complications such as nausea and the potentially serious allergic reactions to dyes make angiography an unsuitable technique for widespread ophthalmic screening applications. In addition, the axial depth resolution requires stereoscopic viewing, which is difficult to demonstrate and teach using routine digital projection strategies.

The rise of OCT for routine clinical evaluations over the past decade has revolutionized the field of ophthalmology by providing unprecedented clinically useful information to aid the diagnosis and treatment of eye diseases. In contrast to the imaging techniques such as FA and ICGA, OCT provides a noninvasive approach to rapidly assess 3-D high-resolution microstructural information of the retina. While the clinical use of OCT has increased tremendously over the past decade, the use of traditional imaging strategies such as FA and FP have declined commensurately.[3] In a recent study, Schneider et al. analyzed compensation-claim data from a managed-care network to assess the trends of relative use of different imaging modalities including OCT, FA and FP from 2001 to 2009.[3] Their analysis concluded that while the frequency of undergoing OCT increased manifolds, the odds of receiving FA decreased by 68% for patients with neovascular AMD. Similar trends were observed for patients with macular edema. While these numbers clearly point to the increased reliance on the use of OCT for diagnosis and management of ocular diseases, FA and ICGA still remain the gold standards for the diagnosis of ocular vasculopathies. However, if OCT imaging could provide structural and functional information about the retinal and choroidal microvasculature, then the preeminence of FA and ICGA could be challenged.

The diagnostic capability of OCT can be significantly enhanced if it can also provide functional information such as blood flow, in addition to the typical 3-D structural details. Doppler-OCT has been used for blood flow imaging, utilizing the well-known Doppler

effect of signals backscattered from moving particles.[4, 5] However, the inherent disadvantage of the angle-dependence of the Doppler phenomenon has prevented it from becoming a reliable clinical tool for imaging retinal blood flow. To mitigate this problem, OCT-based microangiography (OMAG) was recently proposed for the functional *in vivo* imaging of the microvascular network within tissue beds.[6–10] OMAG utilizes OCT signal fluctuation due to moving particles (e.g. red blood cells) as the contrasting mechanism for imaging functional flows. Such method is not sensitive to the angle effect as experienced in Doppler-based flow measurements. In recent years, OMAG has been successfully applied to map functional vascular networks in retina and choroid using SD-OCT systems operating at 800 nm[7, 8] and 1050 nm[11] wavelength ranges. Recently, aided by rapid developments in the swept-source technology, there has been an active research interest in exploring SS-OCT systems at 1 μm wavelength range for imaging the posterior segment of eye. SS-OCT based systems at 1 μm offer the advantages of improved sensitivity roll-off and increased penetration depth into the choroidal tissue.[12]

The objective of the current study is to demonstrate the feasibility of 100 kHz SS-OCT to achieve OMAG imaging of the retinal microvasculature. In addition, we propose to use a stepped-repeated B-scan pattern in the slow scanning direction and an algorithm that utilizes a simple intensity subtraction between repeated B-frames to perform OMAG. The use of intensity differentiation based methods has practical advantages over complex differentiation, as it requires less data storage and post-processing efforts. We evaluate the quality of the retinal OMAG images acquired in normal subjects. We show that the 100 kHz 1050-nm SS-OCT system is capable of obtaining useful retinal OMAG images and has the potential to provide valuable clinical information for the management of retinal microvascular diseases.

MATERIALS AND METHODS

System setup, subject and test procedures

The data were acquired using a modified Cirrus prototype with a swept source laser provided by Carl Zeiss Meditec, Inc. (Dublin, CA, USA) with a central wavelength of 1050 nm (1000–1100 nm in full width) and a speed of 100,000 A-scans per second. Normal subjects were recruited in the current study. The study was approved by the Institutional Review Board (IRB) of the University of Miami and consent form was obtained from each subject before examination. Before data acquisition, each subject was asked to fixate on a point in the center of their view to minimize eye saccades and accommodation during the scanning. The basic adjustment for an eye scan is described as follows: after the head was fixed in the chin-cup, the distance between the eye and the OCT scanner was adjusted for a better view of the iris and the center of the pupil was identified; correction for the refractive error was introduced to focus the beam on the retina; after that, the scan region of interest (ROI) was selected and OCT signal was optimized by using the reference mirror position adjustment and polarization controls; finally, the OCT data were acquired and saved for off-line analysis.

Scanning protocols

A multiple B-mode scan protocol was used to acquire volumetric datasets for OMAG, which were a series of repeated B-scans acquired at the same position over the slow scan direction (Figure 1). For each B-scan, the number of A-scans (m) was 300 covering a lateral distance of ~3 mm in the retinal region. The direction of the B-scan is called as the fast scan direction (*x*). In the slow scan direction (*y*), the scan was stepped 300 times through a range of 3 mm. At each step, B-scans were repeated 4 times in the current study for extracting the flow signal (Figure 1). The time difference between two successive B-scans was roughly 3.8 ms, corresponding to a rate of approximately 263 B-scans per second. Based on this scan protocol and system speed, the total time for a single volume acquisition was about 4.5 s, not including the adjustment time before data collection.

Data processing algorithm

An OMAG algorithm was used to extract the blood flow signals. Figure 2 shows the flowchart for processing the OCT data to generate the final *en face* vasculature distribution image. The original OMAG technique utilized the complex OCT signal, and is described in detail elsewhere.[7, 8] Briefly, complex OCT signals are first obtained by fast Fourier transformation of the dispersion-compensated *k*-space spectral data. Then, significant displacement occurring between adjacent B-scans caused by the involuntary movement of the human eye or head is compensated for by using a 2-D cross correlation method. Further compensation of sub-pixel small motions of the eye might be achieved by using a high order phase compensation scheme as described in a previous publication,[8] if necessary. Finally, a direct differentiation of OCT signals between two consecutive B-scans is calculated and averaged for all repetitions to detect the signal change induced by the blood flow:

$$F(x,z)=\frac{1}{R-1}\sum_{i=0}^{R-1}|C_{i+1}(x,z)-C_i(x,z)| \quad (1)$$

where *i* is the index for the repeated time of B-scans at each *y*-scan position, *x* is the fast axis scan position, *z* is the depth, *C* is the motion corrected complex OCT signal and *R* is the number of repeated B-scans in each step. The complex differentiation based algorithm described above demands a significant amount of post-processing efforts due to the larger complex database and the execution of high-order phase compensation steps. These post-processing efforts require costlier hardware or result in compromises to the workflow efficiency due to much longer processing times, thereby making it less desirable for commercial OCT systems in clinical applications. To mitigate this problem in the current study, we proposed a strategy to contrast blood flow by directly performing differentiating operations of the OCT signal magnitudes between adjacent B-scans, i.e.

$$F(x,z)=\frac{1}{R-1}\sum_{i=0}^{R-1}|I_{i+1}(x,z)-I_i(x,z)| \quad (2)$$

where $I(x, z) = |C(x, z)|$ indicates the amplitude of the complex signal. In this case, the algorithm would be much more efficient in terms of computational power for calculating the flow signals, thereby making it a more practical solution for the clinical use of OMAG in

real time applications. In addition, the data sizes are reduced by a factor of two because only intensity information is required.

A semi-automated retinal and choroidal layer segmentation algorithm was developed to segment physiological retinal layers. This algorithm utilized OCT cross-sectional structural images based on the intensity difference between different retinal layers (Figure 3). In this study, the retina was segmented into three layers: the inner retina from ganglion cell layer (GCL) to inner plexiform layer (IPL), the middle retina from inner nuclear layer (INL) to outer plexiform layer (OPL) and the outer retina from outer nuclear layer (ONL) to external limiting membrane (ELM). Thickness of the three retinal layers as defined in this study varies depending on locations, and the average value is about 60~80 μm.[13] The whole choroid was segmented into two layers: choriocapillaris and choroid. In this study, choriocapillaris was defined as a 30 μm thick slab under RPE, which is easily detectable from the OCT structural images (Figure 3A). Choroid was defined as a ~250 μm thick layer below choriocapillaris layer. The segmentation was conducted on the entire volume. The three-dimensional (3-D) retinal structure and microvascular network in each layer were rendered using the Amira 3D software (FEI Visualization Sciences Group, Burlington, MA, USA) and the maximum amplitude projection was used to produce the *en face* images of the retinal vasculature for easy comparison with FP and FA imaging.

RESULTS

Four normal subjects (#1–4, 32 yr male, 56 yr male, 32 yr female and 33 yr female, respectively) without any identified eye pathologies were imaged and OMAG images were generated. Figure 3 shows the typical results of OMAG from the scan region of ~3×3 mm^2 in the macular region from the right eye of Subject #1. A typical cross-sectional image of the structure and the detected flow are shown in Figure 3 (A, B) to indicate the difference between structural and flow images. The *en face* projection images from the retina and choroid are shown in Figure 3 (C–E) to demonstrate the structural and blood vessel information from the macula. Furthermore, the vascular information from different layers of the posterior eye can be combined and displayed using a single color-coded layer projection vasculature map (Figure 4).

The intensity signal differentiation method used in this study generated capillary-level resolution *en face* OMAG images of the retina from all the subjects. The parafoveal capillaries were clearly visible, thereby allowing visualization of the foveal avascular zone (FAZ). The diameter of FAZ was found to be 588 ± 104 μm in size calculated as a mean value in the nasal-temporal and superior-inferior directions. A vascular ring is found around the FAZ and the capillary vascular density appears to increase radially with the increase of its distance to the foveal center from the color-coded vessel distribution image (Figure 4C and Figure 5). In the choroidal layer, the choriocapillaris layer shows uniform blood perfusion in these normal eyes where the choriocapillaris is located. The detailed structure of choriocapillaris is not visible due to limited lateral resolution of the OCT system; however, in the outer choroidal layer, larger vessels can be seen more clearly. In general, the vascular information disclosed in the choroidal layer seems limited compared to the corresponding retinal layer (see Discussion). All these results correspond well to the

anatomy of vasculature in the posterior eyes in standard textbooks.[14] In order to appreciate the high quality OMAG images that can be achieved using the current system, the microvascular networks from the retinal layers of both eyes from three other normal subjects is shown in Figure 5. Saccades of the eye during imaging can be clearly observed as horizontal white strips in the images. However, despite the motion artifacts, one could clearly observe the inner microvascular ring around the FAZ as well as the capillary level resolution in the OMAG images. All these results show that by using the current system, scan protocol, and OMAG computation algorithm, angiography of the retinal vasculature can be readily achieved.

DISCUSSION

In this study we report some preliminary results of retinal OCT angiography using an intensity differentiation based OMAG algorithm. The data were acquired from normal subjects using a ZEISS 1 μm SS-OCT prototype system with a scanning speed of 100 kHz. The depth-resolved vascular images obtained using the OMAG technique in normal subjects provided detailed information related to the microcirculation network of the retina with a good correspondence to its anatomy, indicating its potential as a clinical tool to study the microvasculature-related diseases of the retina.

A scan mode of 300×300 (*x*: m = 300, *y*: n = 300) with R = 4 at each *y* scan position was adopted in the current study to cover a region measuring 3×3 mm^2, i.e. about 10° angle of view. With a fixed A-scan acquisition speed, number of A-scans per B-scan, number of repetition at each position, and total acquisition time, there was a balance struck between the scan width (*x*) and the scan length (*y*). The scan width could be enlarged but then the number of A-scans per B-scan would need to be increased; otherwise a decrease of spatial resolution would result in degradation of the OMAG quality. The current scan protocol was an optimized solution based on the configuration of the current OCT system.

The segmentation of different layers of the retina in OMAG should be useful for the study of different retinal diseases. For example, most of the vascular changes in diabetic retinopathy (DR) occur in the retinal microvasculature while in AMD, most of the early vascular changes are thought to occur in the choroidal microvasculature while the later neovascular changes might occur in the retina, under the retina, or in the choriocapillaris and subRPE space. It should be noted that the segmentation scheme described in this report cannot be applied uniformly for studying different categories of diseases and therefore, the segmentation scheme may be modified or adapted for a given disease to better aid in diagnosis and disease monitoring. Since no vasculature exists in the outer retina in normal eye, the outer retina is neglected in displaying OMAG images in the current study. However, this layer should be included if any abnormal vascular change is suspected to be existent in this layer when studying macular diseases.

In the OMAG images, the blood vessels including capillaries could be observed clearly in the retinal layer of the fovea. OMAG is an ideal tool for studying the vascular diseases in the retinal layer. However, the vasculature information that can be obtained from the choroidal layer seemed quite limited. The choriocapillaris cannot be seen clearly, which may be due to

the fine structure of the choriocapillaris and limited imaging resolution of the current OCT system. In general, it is more challenging to achieve high resolution choroidal vasculature images. The reasons for poor choroidal vasculature imaging include firstly the attenuation and scattering effect from the RPE layer, which blocks a significant portion of the optical energy entering into the choroidal layer. The second reason is the decorrelation tail effect from the blood vessels lying on the pathway of the light beam above the choroidal layer of interest. The third reason for the degradation in image quality may be related to the increase of multiple scattering signals with greater depth in tissue. However, the situation in patients might be quite different compared to normal subjects when the RPE is altered as in some diseases such as geographic atrophy in dry AMD or pathologic myopia or when the lesion is located in the junction between the retina and choroid such as neovascularization in AMD.

The microcirculation of the retina is critically important for the metabolism which keeps the normal function of vision. In normal subjects, the vascular bed has a high capillary density (as shown in Figure 4 and Figure 5) in order to meet the high metabolic demand of the retinal tissue. Capillary loss or drop-out in the retina may lead to reduced oxygen diffusion into the retinal tissue causing tissue hypoxia. Based on the clear visualization of the absence of capillaries in the FAZ region in normal eyes, it is expected that OMAG might be able to detect regions of flow impairment and ischemia within the retina and detect an increased perifoveal inter-capillary area as well as an increased foveal avascular zone size as previously described in the progression of DR.[15] Furthermore, in the very late stage of DR, there is a proliferation of the retinal neovascularization which might be detectable using OMAG imaging. Consequently, the current OMAG technique, with its capability to provide capillary level retinal imaging may develop into a useful tool to study the early retinal microvascular changes in patients with diabetes mellitus. Macular telangiectasia type 2 (MacTel2)[16] can serve as another good example for demonstrating the clinical value of OMAG.[17] The depth resolved capability of OMAG imaging for blood vessels can be used to detect the origin and follow the progression of the vascular abnormalities in MacTel2.

In conclusion, we successfully applied the OMAG imaging technique using a ZEISS 1 μm SS-OCT prototype system and a specialized scan protocol. OMAG images clearly show the depth-resolved microvasculature of the retina in all the normal subjects imaged. OMAG has the potential to be used as a clinical tool for studying the vascular related pathology in a wide variety of retinal diseases. In a companion paper in this issue,[17] we applied OMAG to the first clinical study of MacTel2. Interested readers can refer to that paper to appreciate the clinical potential of this technique.

Acknowledgments

This work was supported in part by the grants received from Carl Zeiss Meditec, Inc. (Dublin, CA), the National Eye Institute (R01EY024158), the Macula Vision Research Foundation, an unrestricted grant from Research to Prevent Blindness, NEI core center grant P30 EY014801 to the University of Miami, Department of Defense (DOD-Grant#W81XWH-13-1-0048 ONOVA), Feig Family Foundation, and the Emma Clyde Hodge Memorial Foundation.

Disclosure:

Drs. Huang, Zhang, Thorell, Rosenfeld and Wang received research support from Carl Zeiss Meditec, Inc. Dr. Rosenfeld received research support from Acucela, Advanced Cell Technology, and GlaxoSmithKline, and he is a

consultant for Acucela, Alcon, Bayer, Boehringer Ingelheim, Chengdu Kanghong Biotech, Healios K.K., Merck, Oraya, Roche, Sanofi/Genzyme, and Xcovery Vision.

Drs. An, Durbin, Laron and Sharma are employed by Carl Zeiss Meditec, Inc.

REFERENCES

1. Bennett TJ, Barry CJ. Ophthalmic imaging today: an ophthalmic photographer's viewpoint - a review. Clin Exp Ophthalmol. 2009; 37(1):2–13.
2. Yannuzzi LA, Ober MD, Slakter JS, et al. Ophthalmic fundus imaging: today and beyond. Am J Ophthalmol. 2004; 137(3):511–524. [PubMed: 15013876]
3. Schneider EW, Mruthyunjaya P, Talwar N, et al. Reduced fluorescein angiography and fundus photography use in the management of neovascular macular degeneration and macular edema during the past decade. Invest Ophthalmol Vis Sci. 2014; 55(1):542–549. [PubMed: 24346174]
4. Chen ZP, Milner TE, Dave D, Nelson JS. Optical Doppler tomographic imaging of fluid flow velocity in highly scattering media. Opt Lett. 1997; 22(1):64–66. [PubMed: 18183104]
5. White BR, Pierce MC, Nassif N, et al. In vivo dynamic human retinal blood flow imaging using ultra-high-speed spectral domain optical Doppler tomography. Opt Express. 2003; 11(25):3490–3497. [PubMed: 19471483]
6. Wang RK, Jacques SL, Ma Z, et al. Three dimensional optical angiography. Opt Express. 2007; 15(7):4083–4097. [PubMed: 19532651]
7. Wang RK, An L, Francis P, Wilson DJ. Depth-resolved imaging of capillary networks in retina and choroid using ultrahigh sensitive optical microangiography. Opt Lett. 2010; 35(9):1467–1469. [PubMed: 20436605]
8. An L, Shen TT, Wang RKK. Using ultrahigh sensitive optical microangiography to achieve comprehensive depth resolved microvasculature mapping for human retina. J Biomed Opt. 2011; 16(10):106013. [PubMed: 22029360]
9. Zhi ZW, Qin J, An L, Wang RKK. Supercontinuum light source enables in vivo optical microangiography of capillary vessels within tissue beds. Opt Lett. 2011; 36(16):3169–3171. [PubMed: 21847196]
10. Choi WJ, Reif R, Yousefi S, Wang RK. Improved microcirculation imaging of human skin in vivo using optical microangiography with a correlation mapping mask. J Biomed Opt. 2014; 19(3): 036010.
11. Wang RKK, An L. Multifunctional imaging of human retina and choroid with 1050-nm spectral domain optical coherence tomography at 92-kHz line scan rate. J Biomed Opt. 2011; 16(5): 050503. [PubMed: 21639559]
12. Potsaid B, Baumann B, Huang D, et al. Ultrahigh speed 1050nm swept source / Fourier domain OCT retinal and anterior segment imaging at 100,000 to 400,000 axial scans per second. Opt Express. 2010; 18(19):20029–20048. [PubMed: 20940894]
13. Loduca AL, Zhang C, Zelkha R, Shahidi M. Thickness mapping of retinal layers by spectral-domain optical coherence tomography. Am J Ophthalmol. 2010; 150(6):849–855. [PubMed: 20951975]
14. Henkind, P.; Hansen, RI.; Szalay, J. Ocular circulation. In: Records, RE., editor. Physiology of the Human Eye and Visual System. New York: Harper & Row; 1979.
15. Arend O, Wolf S, Jung F, et al. Retinal microcirculation in patients with diabetes mellitus - dynamic and morphological analysis of perifoveal capillary network. Br J Ophthalmol. 1991; 75(9):514–518. [PubMed: 1911651]
16. Yannuzzi LA, Bardal AMC, Freund KB, et al. Idiopathic macular telangiectasia. Arch Ophthalmol. 2006; 124(4):450–460. [PubMed: 16606869]
17. Thorell MR, Zhang QQ, Huang YP, et al. Swept-source OCT angiography of macular telangiectasia Type 2. OSLI Retina. Submitted for review.

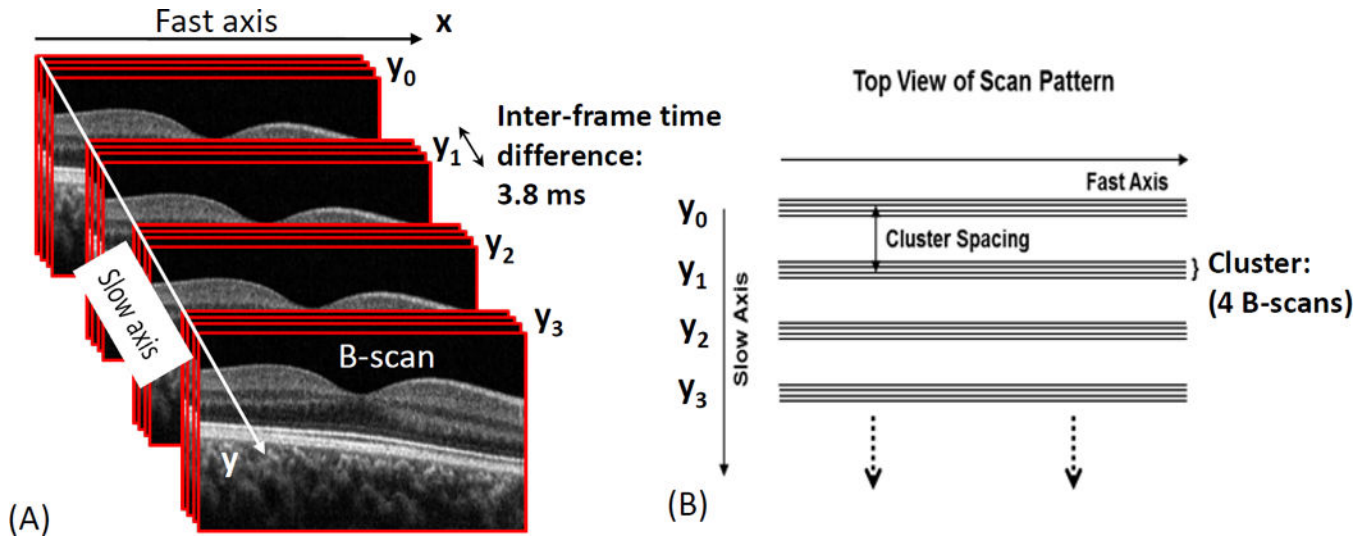

Figure 1.

The scanning protocols for OCT angiography used in the current study. (A) "*x*" indicates the fast axis in a B-scan and "*y*" indicates the slow scan axis, where at each *y* scan point, a cluster of repeated B-scans (4 times in the current study) are performed to extract the flow signal. (B) Top view of the OCT angiography scan pattern: cluster scans comprise of 4 repeated B-scans obtained at the same location.

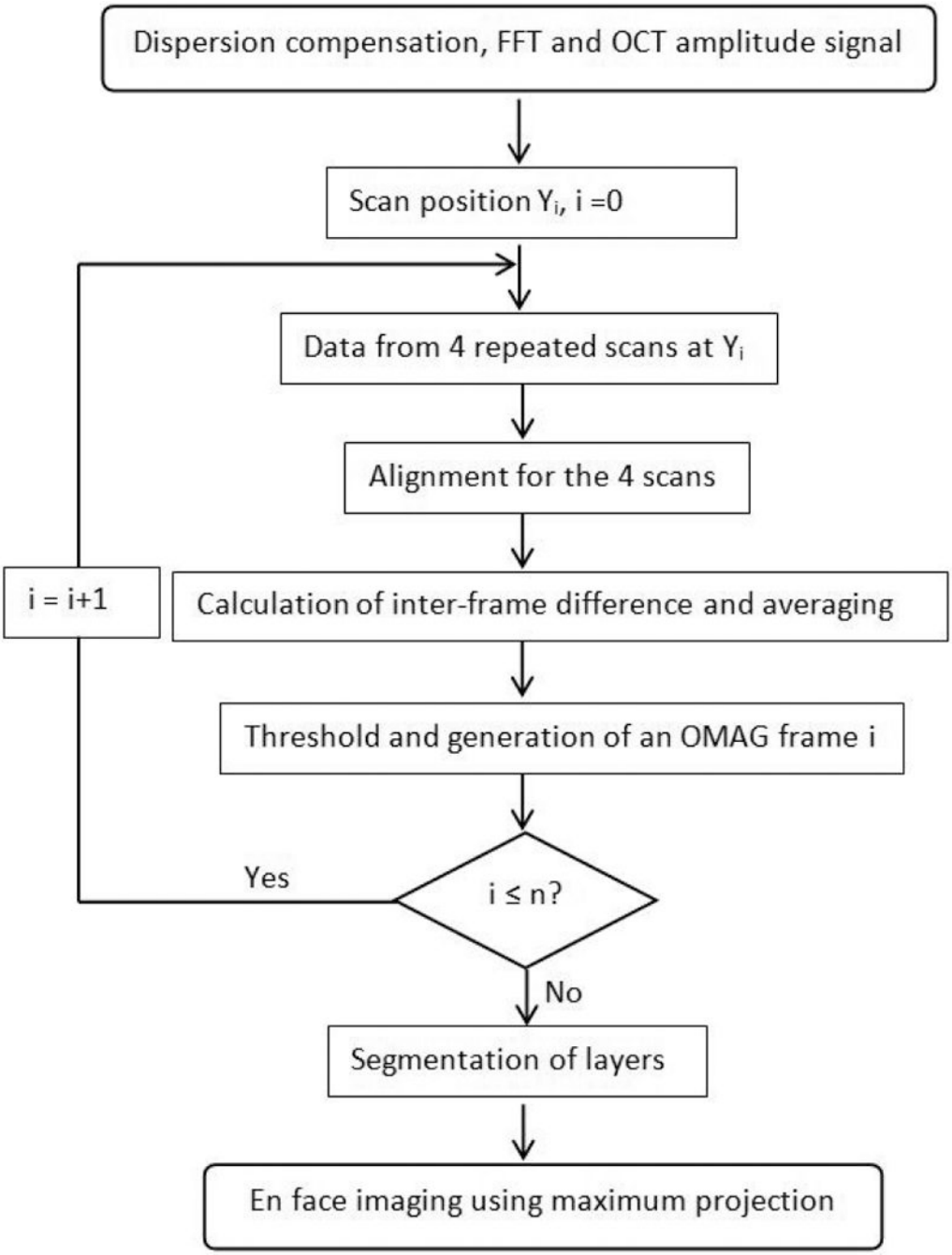

Figure 2.

A flowchart showing OMAG processing steps for generating a projected *en face* vasculature distribution image based on the acquired 3-D volumetric data.

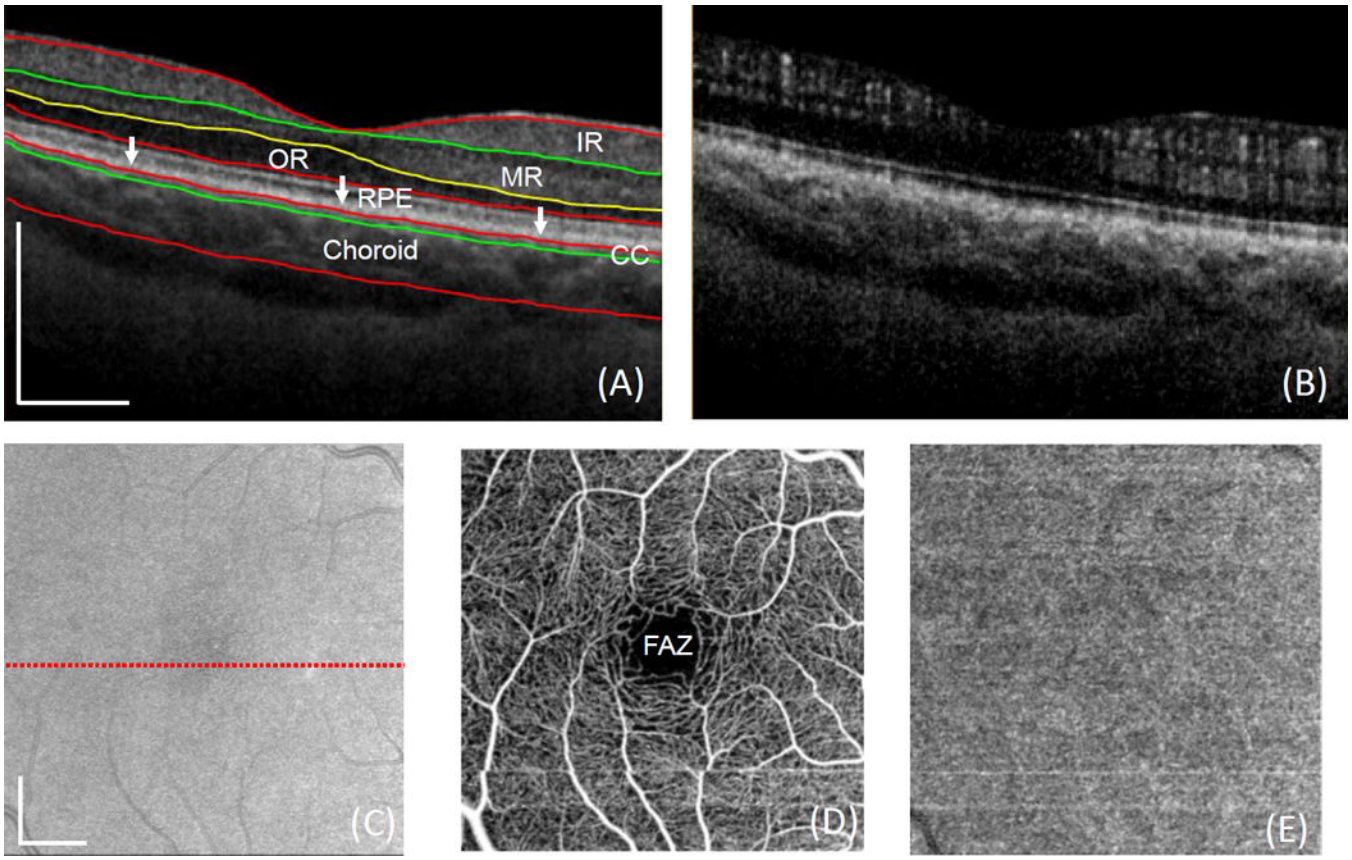

Figure 3.

Typical results of OMAG from a scan region of ~3×3 mm^2 in the right eye of a normal subject (#1). (A) A typical cross-sectional image showing the segmentation lines for the different layers including the inner retina (IR), middle retina (MR), outer retina (OR), choriocapillaris (CC) and choroid. The white arrows in (A) show the RPE layer. (B) OMAG flow image. (C) An *en face* OCT fundus image from the structural OCT signal and the red dotted line shows the location where (A) and (B) are obtained. (D) and (E) show the projected OMAG images for the retinal and choroidal layer, respectively. The scale bars show a distance of 500 μm. FAZ – foveal avascular zone.

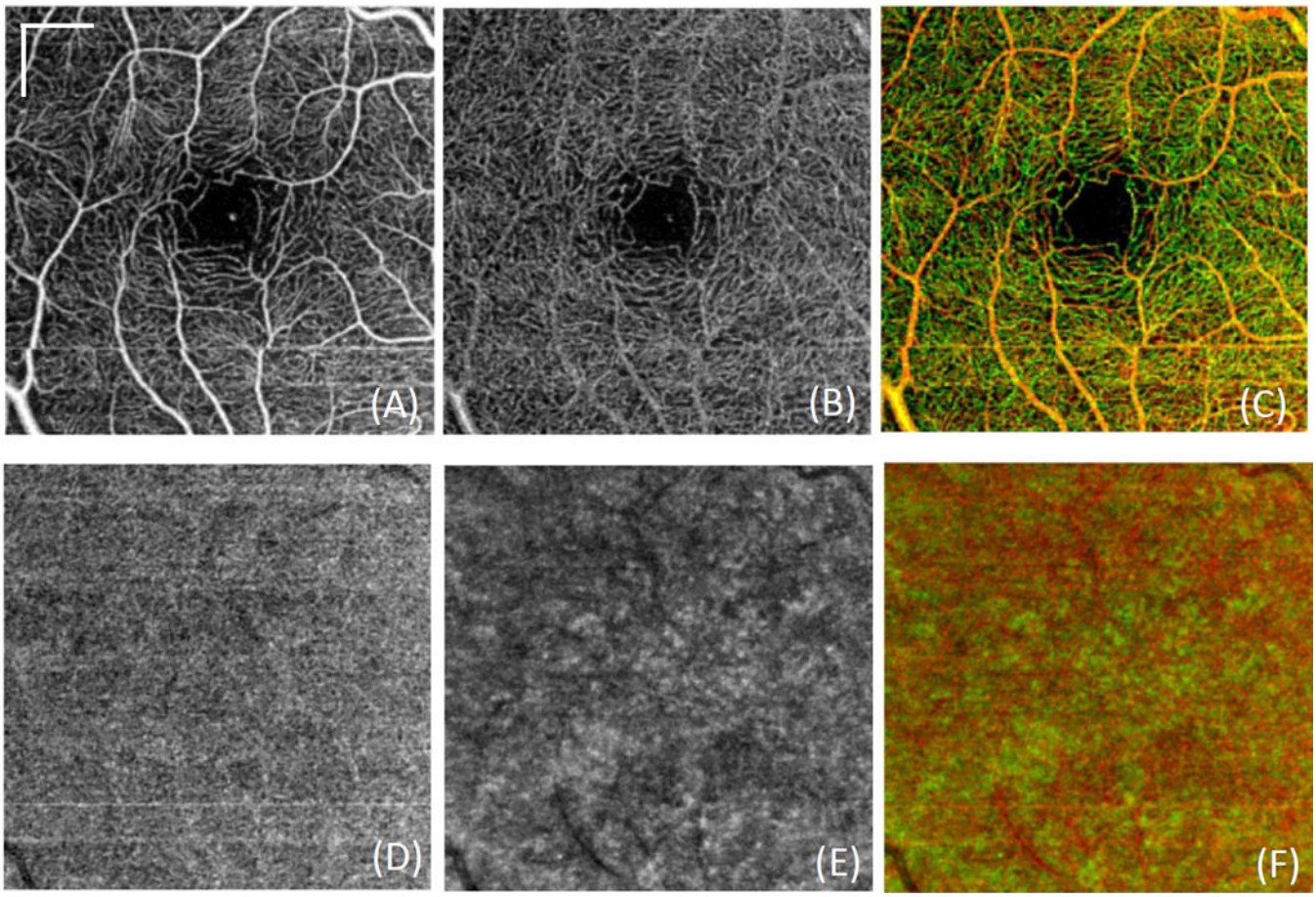

Figure 4.

Typical OMAG images for different lays of retina and choroid in the right eye of Subject #1. (A)–(C) include OMAG images from inner retina, middle retina and the whole retina; (D)–(F) include OMAG images from choriocapillaris, choroid and the whole choroid. In the combined images (C and F), a color coding scheme is used to indicate the blood vessels from different layers. For retina, inner retina = red = ~70 μm of the inner retina, middle retina = green = ~60 μm lying in the middle retina. For choroid, choriocapillaris = red = ~30 μm underneath RPE, choroid = green = ~250 μm underneath choriocapillaris. The scale bars in (A) show a distance of 500 μm which apply to all other images.

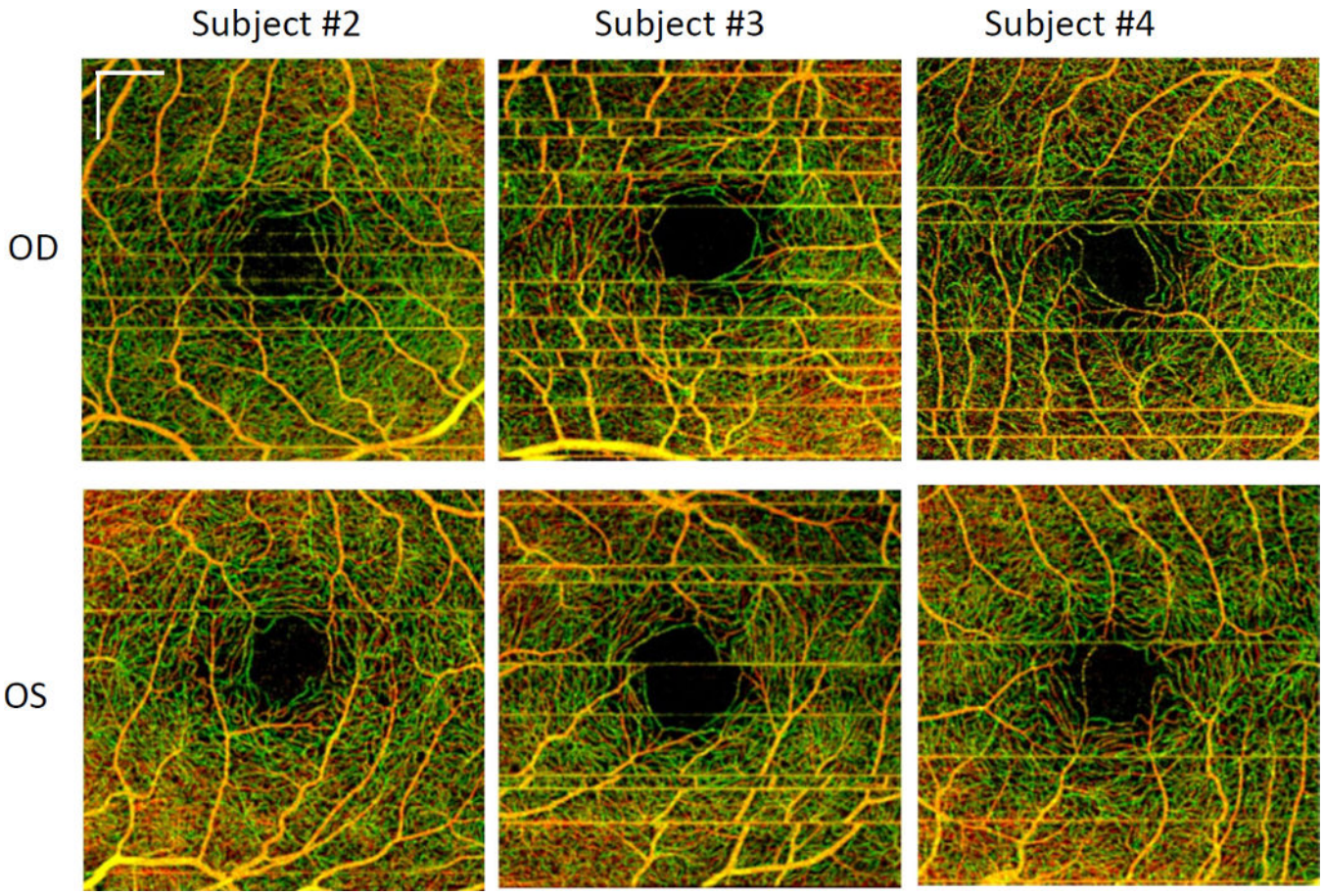

Figure 5.

Color-coded OMAG images of a scanned region of ~3×3 mm^2 in the foveal region from three different normal subjects. Subjects #2–4 are shown for both the right (OD) (top row) and the left (OS) (bottom row) eyes. Color coding: inner retina = red = ~70 μm of the inner retina, middle retina = green = ~60 μm in the middle retina. The scale bars in the first image show a distance of 500 μm which apply to all other images.